Significant reduction of cold temperature extremes at Faraday/Vernadsky Station in the Antarctic Peninsula

Christian Franzke

British Antarctic Survey, Cambridge, UK

Short title: Significant reduction of cold temperature extremes

Keywords: Antarctic warming, Extremes, Faraday station, Vernadsky station

Corresponding author address:
Dr. Christian Franzke
British Antarctic Survey
High Cross, Madingley Road
Cambridge, CB3 0ET
United Kingdom
Phone: +44 (0)1223 221350
Fax: +44 (0)1223 221226

Abstract

This study examines the daily observed temperature at the Faraday/Vernadsky station on the Antarctic Peninsula for the period February 1947 through January 2011. Faraday/Vernadsky is experiencing a significant warming trend of about 0.6°C/decade over the last few decades. Concurrently the magnitude of extremely cold temperatures has reduced while there is no evidence for an increase of the annual maximum temperature.

An empirical mode decomposition reveals that most of the temperature variability occurs on intraannual time scales and that changes in the magnitude of the annual cycle can be explained by a simple periodic stochastic process. Extremely cold temperatures below a threshold follow a Generalised Pareto Distribution (GPD) with a negative shape parameter and thus are bounded. We find evidence that the extreme cold behaviour in the first half of the record is significantly different from the second half. At the same time there is no evident increase of warm temperatures or in the location of the maximum of the temperature probability distribution. These findings provide evidence that at Faraday/Vernadsky it is the change in the shape of the temperature distribution that has substantially contributed to the observed warming over the last few decades.

Furthermore, we find evidence for clustering of extreme cold events and show that they are predictable a few days in advance using a precursor based prediction scheme.

1. Introduction

Although Antarctica is one of the most remote places on Earth, its climate and possible changes in it have potentially strong global impacts. For example, the sea level could rise worldwide by about three meters if the climate were to warm sufficiently to induce a collapse of the West Antarctic ice sheet (Bamber et al. 2009, Joughin et al. 2011). Thus, it is important to understand Antarctic climate variability and change (Thompson and Solomon 2002, King and Comiso 2003, Turner et al. 2005, Chapman and Walsh 2007, Steig et al. 2009, Thomas et al. 2009) and the remoteness of Antarctica allows this to be measured without the effects of other factors such as urban warming (Kalnay and Cai, 2003).

Especially the maritime west coast of the Antarctic Peninsula has experienced some of the most rapid warming worldwide. At Faraday/Vernadsky station a significant warming trend over the last 50 years has been detected (Turner et al. 2005, Steig et al. 2009, Franzke, 2010, 2012) and the Gomez ice core provides further evidence for a significant warming of the Antarctic Peninsula over the last 120 years (Thomas et al. 2009). There is also evidence for warming at the Bellingshausen and Rothera stations, while at most Antarctic stations away from the Peninsula there is no evidence for a significant warming. Halley, Neumayer and the South Pole actually recorded cooling trends; though not at a statistically significant level (Turner et al. 2005, Franzke 2010).

In general, climate change does not only affect the mean temperature but also temperature extremes. The simplest explanation for this is that global warming increases the mean of the temperature but the overall shape of the distribution stays the same. Hence, the maximum of the distribution shifts towards warmer temperatures and the hot extremes increase because the whole distribution is shifted towards warmer temperatures thus increasing the likelihood of hot temperatures. On the other hand, a change in the shape of the distribution can also lead to a change in the mean without a shift in the location of the maximum. If the shape of the distribution would be changed in such a way that the likelihood of cold days is reduced but the likelihood of warm days stays the same, then this would also result in an increase of the mean temperature without a necessary shift in the location of the probability maximum. Both scenarios lead to the same outcome, a warming. But its consequences, especially for ecosystems, can be quite different (Barnes and Peck 2008, Smale et al. 2011).

As discussed in more detail in section 2, there is evidence that the warming trend at Faraday/Vernadsky is accompanied by a reduction in extremely cold temperatures while there is no evidence of a change in maximum temperatures. Thus, the main objective of this study is to disentangle the different components contributing to the observed warming at Faraday/Vernadsky.

In section 2 we introduce the Faraday/Vernadsky temperature time series, in section 3 the time series is decomposed and the statistical significance of its intrinsic modes examined, section 4 presents the results of an extreme value analysis and predictability experiments. A summary is given in section 5.

2. Temperature Data at Faraday/Vernadsky Station

We use daily mean temperature data from the Faraday/Vernadsky station on the Antarctic Peninsula for the period February 1947 through January 2011 from the Reference Antarctic Data for Environmental Research (READER) data set which is quality controlled (Turner et al. 2004, 2005). Faraday/Vernadsky is a station at Marina Point on Galindez Island. The time series has a length of 23376 days. There are a few missing observations of up to 3 consecutive days; most missing observations are just for one day. We used a cubic spline interpolation in order to fill these gaps (Franzke, 2010). The daily mean temperature is displayed in Fig. 1a. A striking feature is the asymmetry of the time series. The warmest temperatures seem to be capped at about 5°-6°C. At the same time a visual inspection of the time series gives the impression that the minimum values are increasing; i.e. that the extreme cold events are less cold over the last few decades. This impression is further strengthened by inspecting annual maxima and minima (Fig. 1b). This shows no evidence for an increase in the magnitude of the temperature maxima over the observation period while the magnitude of the minima seems to have an upward trend and a general reduction in variability. Similar findings for the month of July have been reported by Turner et al. (2011).

In previous studies it has been shown that Faraday/Vernadsky daily mean temperature exhibits a statistically significant trend over at least the last 50 years (Turner et al. 2005, Franzke 2010). But the comparison of the maxima and minima suggest that at Faraday/Vernadsky this warming does not comprise a simple increase of the mean with the shape of the temperature distribution staying the same. If this would be the case one would expect that also the maximum values increase, and we find no evidence for this. This is confirmed by examining the PDFs of the first and second halves of the Faraday/Vernadsky temperature time series separately (Fig. 2). Looking at just the first and second half of the time series separately is the easiest option in order to see if any changes over time have occurred without performing a break point analysis. The maxima of both PDFs are at the same location and the warm temperature distribution is hardly changed. At the same time there is a pronounced reduction of the probability density of extreme cold events from the first to the second half of the time series. The significance of this reduction will be examined below in section 4.

This feature of the Faraday/Vernadsky temperature time series, a reduction of the magnitude of extreme cold events without a concurrent increase in warm events, is somewhat unexpected. Typically one would expect that a significant warming also leads to absolute warmer temperatures and not just to a reduction in cold temperatures.

3. Decomposition of Faraday/Vernadsky Temperature

In order to examine the observed changes in the Faraday/Vernadsky time series in more detail we first use a nonlinear time series method to decompose it into intrinsic modes and then examine their dynamical significance.

3.1 Ensemble Empirical Mode Decomposition

In order to nonlinearly filter the Faraday/Vernadsky temperature time series we use the Ensemble Empirical Mode Decomposition method (EEMD) (Wu et al. 2009, Huang et al. 1998, Huang and Wu 2008, Wu et al. 2007, Qian et al. 2009, Franzke 2010, 2012). EEMD is a noise assisted time series analysis method which decomposes a time series into a finite number of Intrinsic Mode

Functions (IMF) and an instantaneous mean

$$x(t) = \sum_{j=1}^{M} \varphi_j(t) + R(t). \quad (1)$$

The j-th IMF φ can be written in polar coordinates $\varphi_j(t) = r_j(t)\sin(\theta_j(t))$ where r_j is the j-th time dependent amplitude, θ_j the j-th time dependent frequency and R(t) the instantaneous mean. IMFs are different from Fourier modes where both r_j and θ_j are time independent. An IMF is defined by the following two properties (1) each IMF $\varphi_j(t)$ has exactly one zero-crossing between two consecutive local extrema, and (2) the local mean of each IMF $\varphi_j(t)$ is zero. Details about the EMD algorithm are given by Huang et al. (1998) and Huang and Wu (2008).

In order to avoid mode mixing EEMD adds white noise to the observed time series before the sifting process of the standard Empirical Mode Decomposition (EMD) (Huang et al. 1998, Huang and Wu 2008, Wu et al. 2007, Franzke 2010) and treats the mean of the ensemble as the final IMF. We use 1000 ensemble realisations with noise amplitude of 0.5 standard deviations of the original time series. See Wu and Huang (2009) for more details.

3.2 Climate Mode Test

To use EEMD as a nonlinear filtering tool we aggregate the IMFs into an intraannual mode (IMFs with mean periods less than 1 year), a modulated annual cycle (MAC; Wu et al. 2008), interannual mode (IMFs with mean periods between 1 year and 10 years) and decadal mode (IMFs with mean periods larger than 10 years). The residual of the EEMD analysis is the EEMD trend. In order to extract the MAC we follow the procedure of (Qian et al. 2010) by combining IMF8, which contains the annual cycle with a mean period of about 365 days, and IMF9, which contains some annual cycle component as well as interannual variability components. Then we subject them to a single EMD decomposition and the resulting IMF1 is then the MAC (see Figs. 1c and 3a). The remaining IMFs of this decomposition will be added to the interannual mode. As can be seen in Figs. 1c and 3a the MAC has a relative constant mean period of about 365 days and pronounced variations in its amplitude. Starting in the late 1980s the MAC amplitude decreases and its year to year variability is considerably smaller than in the earlier period. As Fig. 3a reveals the MAC tracks very well the annual cycle of the full temperature time series. The MAC also displays variability in its amplitude on longer time scales. The significance of this variability will be tested below.

The intraannual mode explains about 58% and the MAC about 34% of the total variance. Thus, these two modes explain almost all of the variance in the time series, while interannual and decadal scale variability contribute only a minor part. The intraannual mode also reveals the annual cycle of variance (Fig. 3b). The variance increases in the winter and decreases during the summer. This is consistent with the striking differences in the summer and winter season PDFs of Faraday/Vernadsky temperature (Franzke et al. 2012). Fig. 1f reveals that the EEMD trend is nonlinear; i.e. it is not well described by a linear line. This has already been discussed in Franzke (2010, 2012). The temperature time series undergoes also pronounced interannual and decadal scale variations (Fig. 1e and f).

In order to assess the dynamical significance of these modes we compare them with the corresponding modes of an annual periodic autoregressive process of first order (APAR(1)):

$$x_{t+1} = \mu(T) + \alpha(T)x_t + \sigma(T)\zeta_t \qquad (2)$$

where $\mu(T)$ is the periodic mean annual cycle, $\alpha(T)$ denotes the periodic autoregressive parameter, $\sigma(T)$ the periodic standard deviation, ζ_t is a normally distributed white noise variable and T indicates the day of year. The parameters of the APAR(1) model can be easily estimated from data which is not the case for models with a more complex dependence structure like long-range dependence. The parameters in Eq. (2) are estimated from the Faraday/Vernadsky time series by solving the periodic Yule-Walker equations for each T (von Storch and Zwiers 1999). A typical APAR(1) realisation is displayed in Fig. 4. This figure suggests that the APAR(1) model captures the most important aspects of the Faraday/Vernadsky temperature time series: the asymmetry between warm and cold temperature amplitudes and the strong annual cycle. This suggests that a APAR(1) model is a good null model for significance tests for the purpose of this study. We use the same approach as in Franzke (2009) and Franzke and Woollings (2011) to assign statistical significance to the modes.

For this purpose we use a Monte Carlo approach and generate 1000 realisations of the APAR(1) process starting from different initial conditions and with different white noise realisations and subject them to EEMD and then aggregate the IMFs to intraannual, MAC, interannual and decadal modes and then compare whether the energy of the Faraday/Vernadsky modes lies outside the 95 percentile of the APAR(1) ensemble. If this is the case then the Faraday/Vernadsky mode cannot be explained as arising from a simple APAR(1) process and we will then claim that this mode is of dynamical significance.

The climate mode significance test reveals that the intraannual and annual cycle cannot be distinguished from modes produced by a APAR(1) process. The variance of the high-frequency Faraday/Vernadsky mode is 16.7°C^2 while the 95th percentile of the corresponding APAR(1) mode ensemble is 20.8°C^2. The variance of the MAC is 9.8°C^2 while the 95th percentile of the corresponding APAR(1) ensemble MAC is 10.7°C^2. Thus, for these two modes the variance is well inside the APAR(1) variance spread. On the other hand, the interannual and decadal scale variability cannot be explained as arising from APAR(1) climate noise. The interannual Faraday/Vernadsky variance is 1.9°C^2 and outside the 95th percentile of the APAR(1) model value of 1.0°C^2. The same is the case for the decadal mode with a variance value of 0.22°C^2 for the observation and 0.2°C^2 for the APAR(1) model. As already shown in Franzke (2010) Faraday/Vernadsky exhibits a significant trend which cannot be explained as arising from climate noise produced by a APAR(1) process. This suggests that the interannual and decadal variability and the EEMD trend cannot be explained as arising from a APAR(1) model. While there is evidence that the Faraday/Vernadsky time series exhibits a more complex dependence structure as can be captured by the APAR(1) (Franzke 2010) it is likely that the interannual and decadal variability and the trend are caused by intrinsic processes, like oceanic, stratospheric and cryospheric processes, and/or anthropogenic greenhouse gas emissions. In Franzke (2010, 2012) is has been shown that the observed warming trend at Faraday-Vernadsky cannot be explained as arising from long-range dependent climate noise.

4. Extreme Values

In order to examine the statistical behaviour of temperatures exceeding a threshold we fit a Generalised Pareto Distribution (GPD) to the Faraday/Vernadsky temperature time series. The probability density distribution of a GPD is given by:

$$p_{(\xi,\mu,\sigma)}(x) = \frac{1}{\sigma}(1 + \frac{\xi(x-\mu)}{\sigma})^{-\frac{1}{\xi}-1}, x > \mu \quad (3)$$

where ξ denotes the shape parameter, μ the location or threshold parameter and σ the scale parameter. Since extreme value statistics is a theory of maxima we multiply the Faraday/Vernadsky time series by -1 so that the extreme cold temperatures become formally maxima. We use a standard maximum likelihood approach to estimate the scale and shape parameter and uncertainty bounds (Coles 2001). The GPD is generalised in the sense that it contains three special cases: (i) when $\xi > 0$ the GPD is equivalent to an ordinary Pareto distribution, (ii) when $\xi = 0$ the GPD becomes an exponential distribution and (iii) for $\xi < 0$ the GPD is a short-tailed Pareto type II distribution (Coles 2001).

The GPD assumes that the extreme value data are independent. By using daily temperatures this is not the case. However, dependence of the data only influences the scale parameter (Leadbetter et al. 1988) and ultimately the return periods. As shown in Franzke (2010) the Faraday/Vernadsky temperature is long-range dependent. In order to minimise the effect this has on the parameter estimates we decided to decorrelate the data by only using extreme values which are at least 30 days apart. As shown below this decorrelation window is larger than the average cluster size of extreme events. Sensitivity experiments reveal that our results are insensitive to this particular choice of identifying extreme values as long the window is at least larger than the average cluster size of 21 days (see below).

In order to identify the threshold value above which the GPD is a good fit we calculate the mean excess (Embrechts et al. 2001)

$$e(\mu) = \mathbb{E}(X - \mu | X > \mu) \quad (4)$$

If the data X fit a GPD well above a threshold μ then the mean excess function $e(\mu)$ is linear (Embrechts et al. 2001). As Fig. 5a reveals the mean excess function is very well approximated by a linear function below -16°C. (Note that for the purpose of the extreme value analysis the observed time series has been multiplied by -1. Hence, positive amplitude values in Fig. 5 correspond to negative temperatures.) That a GPD is indeed a good fit for values below this threshold is verified by probability plots in the form of quantile-quantile plots (Fig. 5b). The empirical quantiles follow the theoretical GPD quantiles very closely. Thus, the extreme value behaviour of Faraday/Vernadsky is very well captured by an extreme value GPD. Tab. 1 shows that the shape parameter is significantly negative. This indicates that if the extreme cold temperatures indeed follow a GPD they are bounded and cannot reach arbitrarily cold temperatures.

In order to examine if the extreme value behaviour has changed over time we split the time series into two halves and compute the GPD parameters for the first and second halves separately (Tab. 1 and Figs. 5c-f). We have chosen to investigate the first and second half of the time series separately because it is the easiest option and (to the author's knowledge) a break point analysis for GPD hasn't been developed yet. This reveals that the scale parameters are significantly different while the shape parameters are not significantly different. The impact of this change can be highlighted by the corresponding change in the mean value of the corresponding GPD. The mean value of a GPD is given by

$$\mu + \frac{\mu}{1-\xi}, \xi < 1. \qquad (5)$$

This reveals that the mean of the extreme values went up from -22.56°C to -19.06°C; that is by about 3.5°C.

In order to investigate if interannual or decadal scale variability is likely to contribute to this change in extreme value characteristics we repeated the GPD analysis with the EEMD intraannual filtered data (containing only IMFs with mean periods less than 1 year). This analysis again shows that the scale parameters of the two periods are significantly different (Tab. 2). And again the shape parameters are not significantly different. Furthermore, the sign of the shape parameter for the second half is not certain. There is a likelihood that the parameter has changed to zero or a positive value. Computing the mean values of the corresponding GPDs reveal that the mean extreme value is -15.38°C in the first half and -13.49°C in the second half. This is about 2°C.

Taken together, the change in the shape of the PDFs and the GPD parameters between the first and second halves suggests that a substantial part of the observed warming at Faraday/Vernadsky can be explained by a reduction in extreme cold events. It is tempting to compare the warming trend of 3.8°C with the increase in the extreme value mean of about 3.5°C. But then one would compare a change over the whole time span with a change in two data windows.

A fairer comparison is between the climatological means of both halves. The mean in the first half of the time series of -4.6°C increases to -3.0°C in the second half. This suggests that the contribution to warming from the reduction in extreme cold temperatures is partially offset by the increase in the frequency of days with temperatures between -4°C and -7°C (see Fig. 2).

4.1 Clustering of Extremes

Another interesting aspect of the extreme value behaviour is a possible clustering of extreme values. The statistical theory of extreme values assumes that extreme values are independent. But this is rarely the case for environmental variables. Even worse is that extremes can cluster especially if the time series is long-range dependent (Bunde et al. 2005). In Franzke (2010) it has been shown that the Faraday/Vernadsky time series is long-range dependent. Thus it is interesting to see if extremely cold temperatures at Faraday/Vernadsky station tend to cluster.

A clustering of extreme values can be quantified by the extremal index. The extremal index is proportional to the inverse of the average cluster size; i.e. the time length over which one expects extreme values to bunch together. We use the method put forward by Hamidieh et al. (2010) to estimate the extremal index. This approach uses the property that the maxima of blocks of size m are proportional to the extremal index $\theta(j)$ for dyadic block sizes $m=2^j$. If the block size dependent estimates extend over a few blocks the estimate is robust and provides evidence for the clustering of extremes.

Fig. 6 shows that the mean estimates of the extremal index θ(j) in terms of a box plot. The central mark in the box denotes the median estimate. For the scales j=8,..., 11 the central marks have almost the same values and are inside each other's error bounds as given by the edges of the boxes which denote the 25th and 75th percentiles of the estimates. Hence for these scales the extremal index estimate is therefore robust. This is also the largest range of scales over which the extremal index is robust. This suggests that the value of the extremal index is about 0.047 (Fig. 6); thus the average cluster size is approximately 21 days. This suggests that extremely cold periods can last for about 3 weeks. This also justifies the 30 day choice of decorrelating the data in section 3 and suggests that the long-range dependence has a negligible influence on the extreme value behaviour if the data has been sufficiently decorrelated.

4.2 Predictability of Extreme Temperatures

Are extremely cold temperatures predictable or do they just occur by chance? To address this question we use the prediction by precursor approach by Hallerberg et al. (2008) for predicting extremely cold temperatures. Precursors are patterns which typically precede the extreme events. For the purpose of the predictability experiments we define that an extreme event occurs when a threshold is crossed.

In order to determine the precursor we first estimate the probability distribution of values which precede an extreme event. The maximum of this distribution is the precursor. As extreme events we consider all events whose temperature are lower than -16°C; this is the threshold below which the GPD is a good fit to the data and thus values below this threshold can be considered to be extreme events. We estimate the precursors for different lags of 1 to 7 days. We use Receiver-Operator Characteristic (ROC) curves to visualise the predictive skill of the used simple prediction scheme.

A ROC curve is a plot of the true positive (hit rate) against the false positive (false alarm rate) prediction rate as a threshold is varied. The best possible prediction would be located in the upper left corner at point (0,1). This would represent a 100% rate of true positive and 0% rate of false positive predictions. A random guess prediction would be located along the diagonal from the left bottom to the right upper corner. This diagonal line divides the ROC space. Predictions which lie above the diagonal line represent good predictions while points below this line are bad predictions.

In order to compute the ROC curves we vary the distance between the precursor pattern and the temperature at time t from zero in increments of 0.25°C for 50 increments. By doing so we allow for measurement and estimation uncertainty. Furthermore, the probability that the observed temperature has exactly the precursor value goes to zero as distances increases. Hence, we have also to examine how sensitive the predictions are to the distance of the observed temperature to the precursor value. This is efficiently encoded in a ROC curve.

For the predictability study we use a leave-one-out approach. We use one year as the validation data and the remaining years as the training data. We repeat this procedure in such a way that each year is once used as validation data.

As Fig. 7 shows our simple prediction approach produces skilful predictions of extremely cold temperatures. For all lags the ROC curves are well above the diagonal line. The best predictions are achieved for lag 1-day. The prediction skill is gradually decreasing for increasing lags before saturating at about lag 5-days. These results suggest that successful short-term predictions of extremely cold temperatures are possible.

5. Summary and Discussion

A decomposition of the Faraday/Vernadsky temperature time series reveals that it exhibits significant interannual and decadal variations and a nonlinear trend. Furthermore, our analysis reveals that a large part of the observed warming of about 3.8°C is likely due to a decrease in the magnitude of cold temperatures without a comparable increase in warm temperatures. Warm temperatures seem to be bounded. Thus, the most striking effect of the observed temperature at Faraday/Vernadsky is the simultaneous warming trend and the significant reduction in variability which affects almost entirely cold temperatures.

The decrease in extremely cold temperatures is likely related to the observed changes and the trend in the Southern Annular Mode (SAM; Marshall (2003), Franzke (2009)) and/or the observed change in the non-annular atmospheric circulation (Turner et al. 2009). Both changes have been attributed to result from stratospheric ozone depletion (Roscoe and Haigh 2007). Furthermore, global climate projections suggest that the frequency of hot extremes will increase due to global warming (Meehl et al. 2007). Also observations show an increase in hot extremes (e.g. Qian et al. 2011b). Hence, our results are somewhat at odds with the general opinion that global warming leads to more frequent and larger extremes. At least at Faraday/Vernadsky the opposite is the case. This is likely due to its geographical location. The maritime location and the heat capacity of the ocean are likely exerting a damping effect on high temperatures. Thus, the annual maximum temperatures are almost constant over the last six decades. Another factor is likely the orography of the Antarctic Peninsula with a mountain range in the north-south direction. The extreme cold events are typically accompanied by northward winds originating in the interior of the Antarctic continent. On the other hand southward winds will advect warm air. The observed non-annular circulation changes will lead to a preference of southward winds. This suggests that the changes in the non-annular circulation component are causing the reduction in extreme cold events. This might suggest that stratospheric ozone depletion plays a role in the reduction of extremely cold temperatures at Faraday/Vernadsky; similar evidence has been found by Hughes et al. (2007).

A possible explanation was put forward by Qian et al. (2011a) how changes in the annual cycle and a trend can lead to non-symmetric changes in temperatures. Applying their reasoning to our results suggests that the combined effect of the weakening MAC (Fig. 1c) and the long-term warming trend (Fig. 1f), which compete each other in summer but reinforce each other in winter, may play a role in the pronounced reduction of cold temperatures without leading to a increase of warm temperatures. Hence, the amplitude reduction in the annual cycle is reducing cold extremes during winter without increasing warm temperatures during summer.

Acknowledgments

I thank Mervyn Freeman and two anonymous reviewers for their very valuable comments on an earlier draft of this manuscript. This study is part of the British Antarctic Survey Polar Science for Planet Earth Programme. It was funded by The Natural Environment Research Council.

References

Bamber, J. L., R. E. M. Riva, B. L. A. Vermeersen and A. M. LeBrocq: Reassessment of the Potential Sea-Level Rise from a Collapse of the West Antarctic Ice Sheet. Science, 324, 2009. doi:10.1126/science.1169335

Barnes, D. K. A. and L. S. Peck: Vulnerability of Antarctic shelf biodiversity to predicted regional warming. Clim. Res., 37, 149-163, 2008. doi:10.3354/cr00760

Bunde, A., J. F. Eichner, J. W. Kantelhardt and S. Havlin: Long-term memory: a natural mechanism for the clustering of extreme events and anomalous residual times in climate records. Phys. Rev. Lett., 94, 048701. doi: 10.1103/PhysRevLett.94.048701

Chapman W. L. and J. E. Walsh: A Synthesis of Antarctic Temperatures, J. Climate, 20, 4096-4117, 2007.

Coles, S.: An introduction to statistical modelling of extreme values. Springer, 224p, 2001.

Franzke, C.: Multi-Scale Analysis of Teleconnection Indices: Climate Noise and Nonlinear Trends. Nonlin. Pro. Geophys., 16, 65-76, 2009.

Franzke, C.: Long-Range Dependence and Climate Noise Characteristics of Antarctic Temperature

Data. J. Climate, 23, 6074-6081, 2010.

Franzke, C.: Nonlinear Trends, Long-Range Dependence and Climate Noise Properties of Surface Temperature. J. Climate, accepted, 2012.

Franzke, C. and T. Woollings: On the Persistence and Predictability Properties of North Atlantic Variability. J. Climate, 24, 466-472, 2011.

Franzke, C., T. Graves, N. W. Watkins, R. B. Gramacy and C. Hughes: Robustness of estimators of long-range dependence and self-similarity under non-Gaussianity. Phil. Trans. R. Soc. A, in press, 2012.

Embrechts, P., C. Klüppelberg and T. Mikosch: Modelling Extremal Events. Springer, 648p, 2001.

Hallerberg, S., J. Bröckner and H. Kantz, 2008: Prediction of extreme events. Nonlinear Time Series Analysis in the Geosciences. Lecture notes in Earth Sciences, Springer.

Hamidieh, K., S. Stoev and G. Michailidis, 2010: On the estimation of the extremal index based on scaling and resampling. J. Comp. Graphical. Stat., 18, 731-755.

Huang, N. E., Z. Shen, S. R. Long, M. C. Wu, H. H. Shih, Q. Zheng, N.-C. Yen, C. C. Tung and H. H. Liu, 1998: The Empirical Mode Decomposition and the Hilbert Spectrum for Nonlinear and Non-Stationary Time Series Analysis. Proc. R. Soc. Lond. A, 454, 903-995.

Huang, N. E. and Wu, Z.: A Review on Hilbert-Huang Transform: Method and its Applications to Geophysical Studies. Rev. Geophys., 46, 2008. RG2006, doi:10.1029/2007RG000228

Hughes, G. L., S. S. Rao and T. S. Rao: Statistical analysis and time-series models for minimum/maximum temperatures in the Antarctic Peninsula. Proc. R. Soc. A, 463, 241-259, 2007.

doi:10.1098/rspa.2006.1766

Joughin, I. and R. B. Alley: Stability of the West Antarctic ice sheet in a warming world. Nature Geoscience, 4, 2011. doi: 10.1038/NGEO1194

Kalnay, E. and M. Cai: Impact of urbanization and land-use change on climate. Nature, 423, 528-531, 2003.

King, J. C. and J. C. Comiso: The spatial coherence of interannual temperature variations in the Antarctic Peninsula. Geophys. Res. Lett., 30, 1040, 2003. doi: 10.1029/2022GL015580

Leadbetter, M. R. and H. Rootzen: Extremal theory for stochastic processes. Ann. Prob., 16, 431-478, 1988.

Rilling, G., Flandrin, P. and Goncalves, P.: On Empirical Mode Decomposition and Its Algorithms. IEEE-EURASIP Workshop on Nonlinear Signal and Image Processing NSIP-03. GRADO(I), 2003.

Qian, C., C. Fu, Z. Wu and Z. Yan: On the secular change of spring onset at Stockholm. Geophys. Res. Lett, 36, L12706, 2009. DOI:10.1029/GL038617

Qian, C., Z. Wu, C. Fu and T. Zhou: On multi-timescale variability in China in Modulated annual cycle reference frame. Adv. Atmos. Sci., 27, 1169-1182, 2010. DOI:10.1007/s00376-009-9121-4

Qian, C., Wu, Z., C. Fu and D. Wang: Changes in the amplitude of the temperature annual cycle in China and their implication for climate change research. J. Climate, 24, 5292-5302, 2011a.

Qian, C., Yan, Z., Wu, Z., Fu, C. and Tu, K.: Trends in temperature extremes in association with weather-intraseasonal fluctuations in Eastern China. Adv. Atmos. Sci., 28, 297-309, 2011b.

Marshall, G. J.: Trends in the Southern Annular Mode from Observations and Reanalyses. J. Climate, 16, 4134-4143, 2003.

Meehl, G. A., et al., 2007: Global Climate Projections. In: Climate Change 2007: The Physical Science Basis. Contribution of Working Group I to the Fourth Assessment Report of the Intergovernmental Panel on Climate Change [Solomon, S. D. et al. (eds.)] Cambridge University Press, Cambridge, United Kingdon and and New York, NY, USA.

Roscoe, H. K. and J. D. Haigh, 2007: Influences of ozone depletion, the solar cycle and the QBO on the Southern Annular Mode. Q. J. R. Meteorol. Soc., 133, 1855-1864. doi: 10.1002/qj.153

Smale, D. A., T. Wernberg, L. S. Peck and D. K. A. Barnes: Turning on the heat: Ecological response to simulated warming in the sea. PLoS ONE, 6, e16050, 2011. doi: 10.1371/journal.pone.0016050

Steig, E. J., D. P. Schneider, S. D. Rutherford, M. E. Mann, J. C. Comiso and D. T. Shindell: Warming of the Antarctic Ice-Sheet Surface since the 1957 International Geophysical Year. Nature, 457, 459-462, 2009.

Thomas, E. R., P. F. Dennis, T. J. Bracegirdle and C. Franzke: Ice core evidence for Significant 100 year regional warming on the Antarctic Peninsula. Geophys. Res. Lett., L20704, 2009. doi:10.1029/2009GL040104.

Thompson, D. W. J. and S. Solomon: Interpretation of Recent Southern Hemisphere Climate Change. Science, 296, 895-899, 2002.

Turner, J., S. R. Colwell, G. J. Marshall, T. A. Lachlan-Cope, A. M. Carleton, P. D. Jones, V. Langun, P. A. Reid and S. Iagovkina: The SCAR READER Project: Toward a High-Quality Database of Mean Antarctic Meteorological Observations. J. Climate, 17, 2890-2898, 2004.

Turner, J., S. R. Colwell, G. J. Marshall, T. A. Lachlan-Cope, A. M. Carleton, P. D. Jones, V. Langun, P. A. Reid and S. Iagovkina: Antarctic Climate Change During the Last 50 Years. Int. J. Climatol., 25, 279-294, 2005.

Turner, J., J. C. Comiso, G. J. Marshall, T. A. Lachlan-Cope, T. Bracegirdle, T. Maksym, M. P. Meredith, Z. Wang and A. Orr: Non-annular atmospheric circulation change induced by stratospheric ozone depletion and its role in the recent increase of Antarctic sea ice extend. Geophys. Res. Lett., 36, L08502, 2009. doi: 10.1029/2009GL037524

Turner, J., T. Maksym, T. Phillips, G. J. Marshall and M. P. Meredith: The impact of changes in sea ice advance on the large winter warming on the western Antarctic Peninsula. Int. J. Climatol., in press, 2011.

Von Storch, H. and F. W. Zwiers: Statistical Analysis in Climate Research. Cambridge University Press. 484pp., 1999.

Wu, Z., Huang, N. E., Long, S. R. and Peng, C. K.: On the Trend, Detrending, and Variability of Nonlinear and Nonstationary Time Series. Proc. Nat. Acad. Sci. USA, 104, 14889-14894, 2007.

Wu, Z., Schneider, E. K., Kirtman, B. P., Sarachik, E. S., Huang, N. E. and Tucker, C. J.: The modulated annual cycle: an alternative reference frame for climate anomalies. Clim. Dyn., 31, 823-841, 2008. Doi: 10.1007/s00382-008-0437-z

Wu, Z. and Huang, N. E.: Ensemble Empirical Mode Decomposition: A Noise-Assisted Data Analysis Method. Adv. Adapt. Data Anal., 1, 1-41, 2009.

Table 1 Parameters of GPD fit to Faraday/Vernadsky temperature time series with 95% uncertainty bounds.

GPD	1947-2011	First Half	Second Half
Shape Parameter	-0.41 (-0.53, -0.29)	-0.49 (-0.62, -0.36)	-0.24 (-0.01, -0.47)
Scale Parameter	10.99 (13.38, 9.03)	14.25 (17.50, 11.60)	7.52 (10.36, 5.46)
Threshold	16.00	13.00	13.00

Table 2 Parameters of GPD fit to EEMD high-frequency filtered Faraday/Vernadsky temperature time series with 95% uncertainty bounds.

GPD	1947-2011	First Half	Second Half
Shape Parameter	-0.35 (-0.49, -0.21)	-0.46 (-0.61, -0.31)	-0.23 (-0.48, 0.02)
Scale Parameter	6.39 (5.24, 7.82)	7.86 (6.26, 9.86)	4.29 (3.00, 6.16)
Threshold	10.00	10.00	10.00

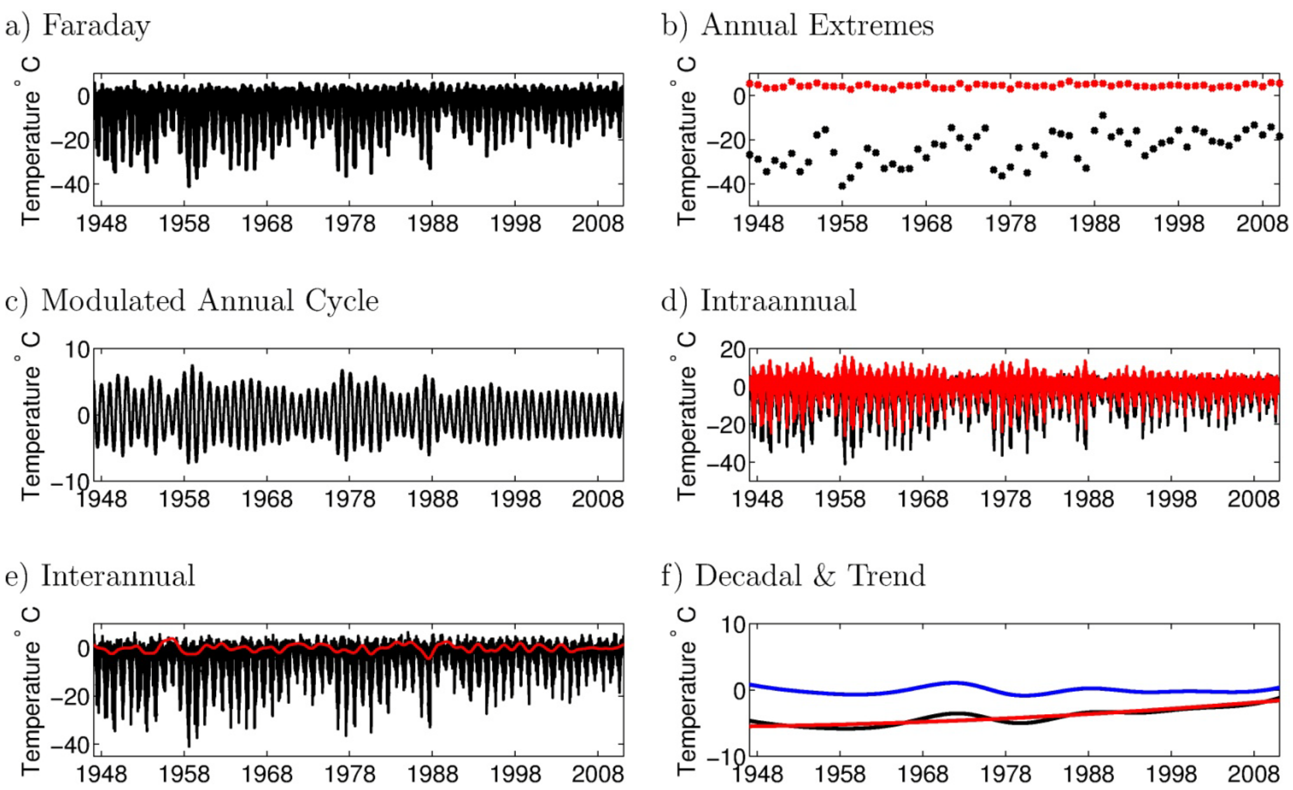

Figure 1 a) Daily Faraday/Vernadsky temperature time series, b) annual temperature maxima (red crosses) and minima (black crosses); c) modulated annual cycle of daily Faraday/Vernadsky temperature; d) intraannual Faraday/Vernadsky station temperature time series (red line) superposed on daily Faraday/Vernadsky temperature time series (black line); e) interannual Faraday/Vernadsky station temperature time series (red line) superposed on daily Faraday/Vernadsky temperature time series (black line) and f) decadal Faraday/Vernadsky station temperature time series (blue line), EEMD trend (red line) and sum of decadal time series and trend (black line).

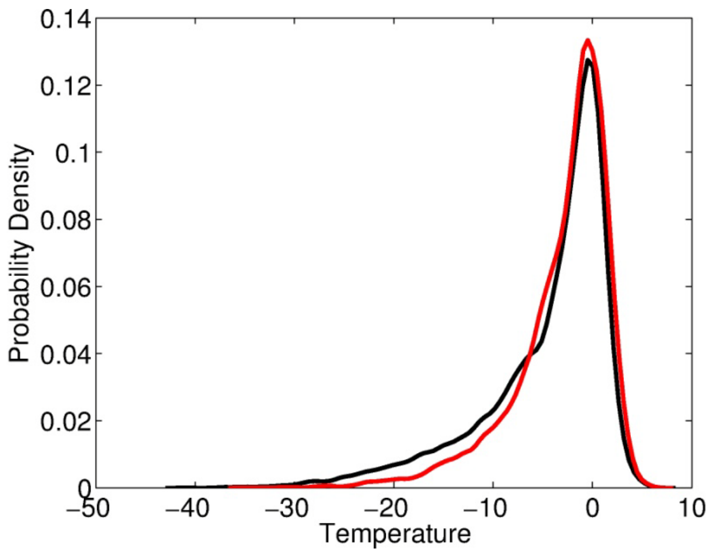

Figure 2 Probability Density Function of Faraday-Vernadsky temperature time series: First half (Black line) and second half (Red line) of time series.

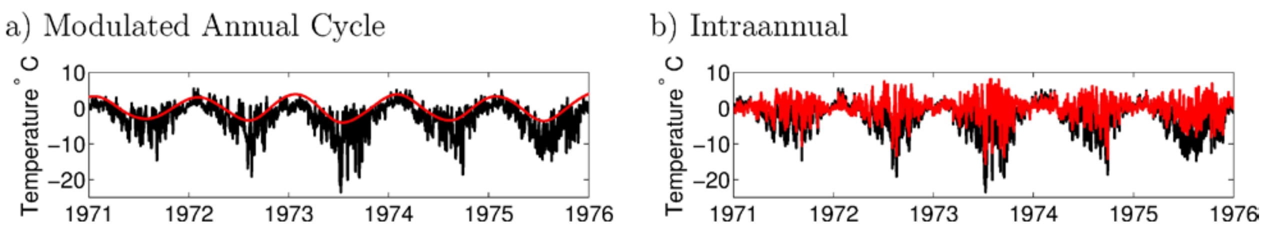

Figure 3: a) Modulated annual cycle of daily Faraday/Vernadsky temperature (red line) superposed on daily Faraday/Vernadsky temperature time series (black line); b) intraannual Faraday/Vernadsky station temperature time series (red line) superposed on daily Faraday/Vernadsky temperature time series (black line) for the period of 1971 through 1975.

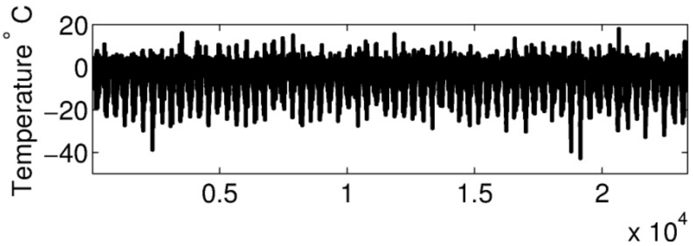

Figure 4 A typical realisation of the APAR(1) model fitted to Faraday/Vernadsky temperature time series.

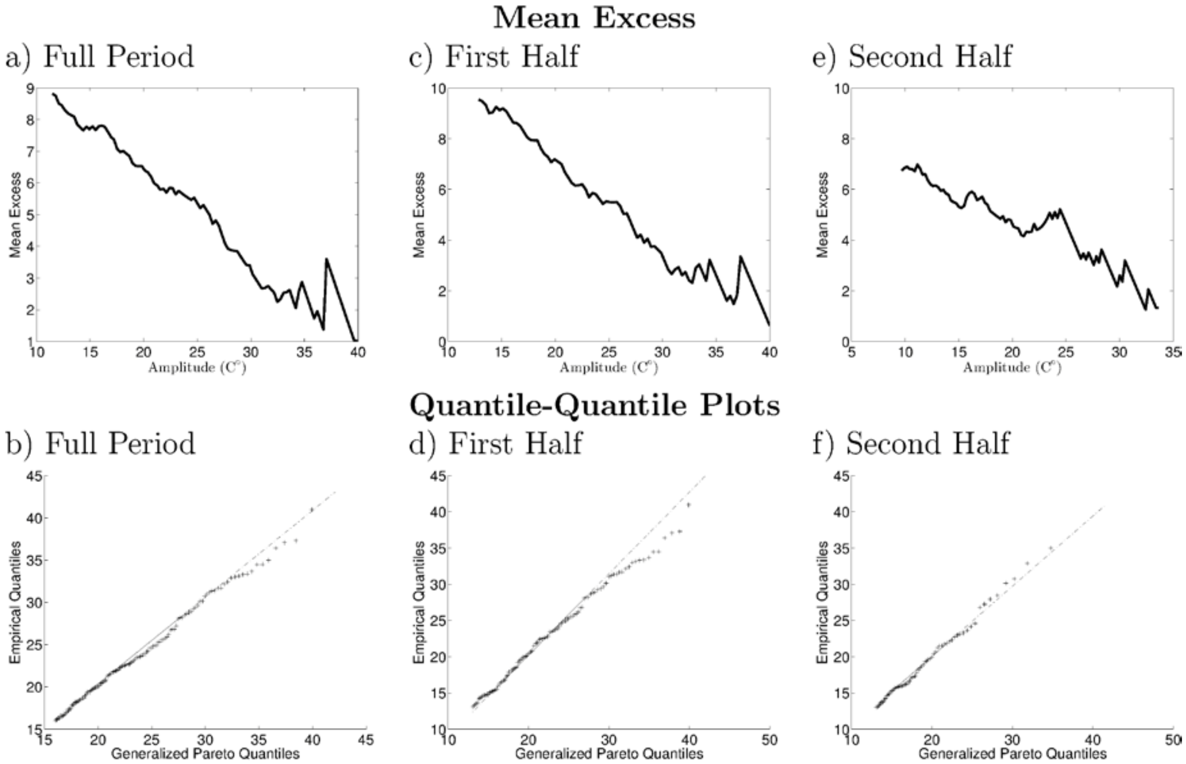

Figure 5 Mean excess function (upper row) and quantile-quantile plots (lower row) of Faraday/Vernadsky temperature. Note that for the purpose of the extreme value analysis the observed time series has been multiplied by -1. Hence, positive amplitude values correspond to negative temperatures.

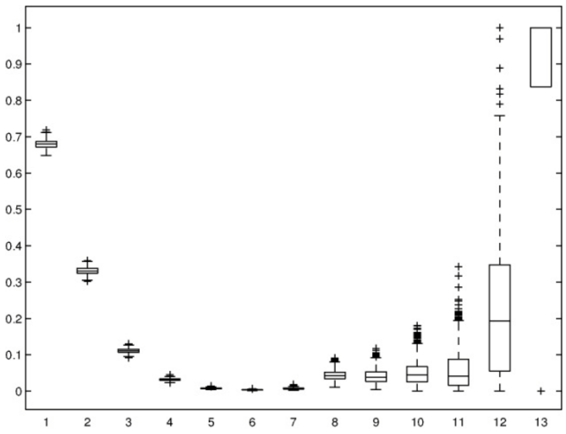

Figure 6 Box plots of the θ(j) obtained from bootstrapped estimates. The central mark in the box is the median estimate, the edges of the boxes are the 25th and 75th percentiles, the whiskers extend to the most extreme estimates not considered to be outliers and the crosses indicate individual outliers.

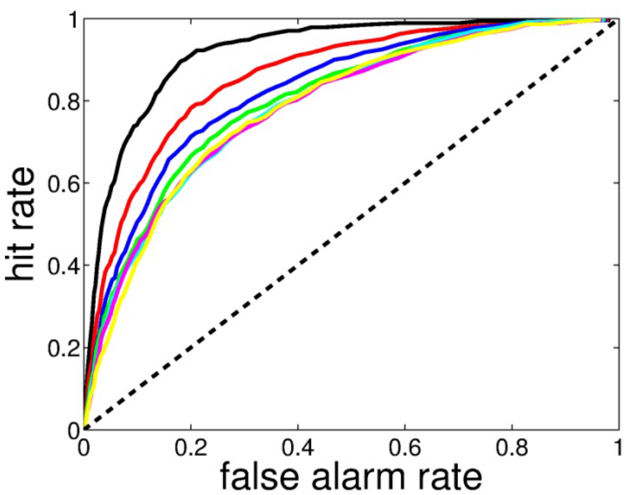

Figure 7 Receiver-Operator Characteristics (ROC) curve. 1-day lag (black), 2-day lag (red), 3-day lag (blue), 4-day lag (green), 5-day lag (cyan), 6-day lag (magenta) and 7-day lag (yellow).